ACADEMIA ROMÂNĂ
Revue Roumaine de Chimie
http://web.icf.ro/rrch/

Rev. Roum. Chim.,
2020, *65*(2), 135-140
DOI: 10.33224/rrch.2020.65.2.02

SMALL-ANGLE X-RAY POWDER DIFFRACTION ANALYSES, MICROSTRUCTURE AND MORPHOLOGY OF SOME SYNTHESIZED TEMPLATE SILICA SAMPLES RELATED TO THE 2-METHOXYETHANOL CONTENT

Ana-Maria PUTZ,[a,*] Jiri PLOCEK,[b] Petr BEZDICKA[b] and Cecilia SAVII[a]

[a]Institute of Chemistry Timişoara of Roumanian Academy, Bv. Mihai Viteazul, No.24, RO-300223 Timişoara, Roumania
[b]Institute of Inorganic Chemistry of the Czech Academy of Sciences, Husinec-Řež 1001, 25068 Řež, Czech Republic

Received July 31, 2017

A series of mesoporous silica materials have been synthesized by using a high alcohol concentration in order to structurally characterize them, with the aid of the Small-angle X-ray Powder Diffraction (XRD) method. A short-range ordered pore structure was obtained, mainly attributed to hexagonal pore symmetry or to a coexistence of cubic and hexagonal arrangements.

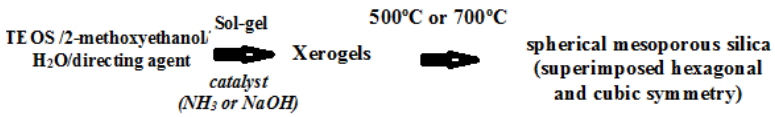

INTRODUCTION

Monodispersed mesoporous silica spheres with tuneable particle size and porosity can be synthesized from TEOS and CTAB under alkaline conditions.[1] The CTAB molecules are partitioning at the TEOS-water interface, where the hydrolysis and condensation of TEOS are promoted.[2] Besides the directing agent role, the CTAB favours also the TEOS solubilisation, as accelerates the hydrolysis of TEOS to form soluble TEOS species.[2] Ordered mesoporous spherical silica particles have been obtained by using n-alkyl trimethyl ammonium bromides with different chain length as surfactants.[3] Thus, mesoporous materials MCM-41 with the hexagonal arrangement of pores were obtained using dodecyltrimethylammonium bromide (C12) and octadecyltrimethylammonium bromide (C18) as templating surfactants, besides the well-known used templating agent, CTAB (C16).[4] Different chain lengths have been employed in another study too, to get different pore sizes.[5] Also, the morphology of the silica particles depends on surfactant alkyl chain length[6]. Another factor which is influencing the structure is the concentration of the alcohol added into the reaction mixture. By combining diffraction methods with electron microscopy methods, Pauwels's, Lebedev's, Van Tendeloo's and Liu's groups have demonstrated that: the regular hexagonal MCM-41 was obtained when (EtOH) was absent in the reactant mixture. Corresponding to the EtOH : TEOS molar ratio of 20 :1, the cubic MCM-48 type of silica resulted. Eventually, by increasing the EtOH : TEOS molar ratio up to 58:1 the MCM-41 type of ordered structure was obtained. The same authors showed that, in the last case the specific XRD structure, for the obtained spherical silica actually consisted in a mixture of hexagonal and cubic arrangements.[7] Owing the alcohol amount addition to the synthesis of a mesoporous silica material, a transition from

* Corresponding author: putzanamaria@acad-icht.tm.edu.ro

hexagonal (MCM-41) to cubic (MCM-48) to lamellar phase was inducing because the alcohol adopts the role of co-surfactant.[8-11] The higher alcohol concentration (TEOS: EtOH=1:58), apparently not only affects the pore ordering, but also influences the morphology of the particles. In the continuation of these studies, the purpose of the present work was to analyse further these kind of systems, actually consisting of cubic and hexagonal mixed arrangements, by using the small angle X-ray powder diffraction method. We have synthesised a series of samples by using high alcohol concentration (the molar ratio TEOS: alcohol =1:58). Compared with the previous presented studies we changed the alcohol nature, specifically by using 2-methoxyethanol. All series of silica porous samples, as xerogels and as silica matrices obtained by thermally removal of sacrificial templates, were structurally studied by using the Smal –angle X-ray Powder Diffraction. Such way it was analysed the certain factors influencing order-disorder transitions in the mesoporous silica synthesized samples (as xerogels-dried at 60°C or as 500°C or 700°C calcined materials), such as, the side chain length of the used cationic surfactants (CTAB or DTAB), and the use of surfactants equimolecular mixture, (CTAB:DTAB=1:1 mole ratio), taking also into account the influence of chemical environment set by catalyst (NH3 or NaOH).

RESULTS

The X-ray diffraction features assignment and the calculated lattice parameter, for all the analysed materials (the xerogels and calcined samples) are presented in Table 1. In Figure 1 there is presented a selection of the representative diffraction patterns of the samples obtained after the thermal treatment at 500°C (with ammonia or NaOH catalyst). Beside examining the information sourced from the prepared in the work basic silica materials investigations, for us it was of interest to collect and analyse certain ultra-small particle fraction collected by centrifugation from the silica sample supernatants, that was extremely difficult even impossible to be separated by sedimentation or filtration.

We paid attention to the symmetry and mainly we discussed the phase composition of the different categories of samples.

The samples with **cubic structure** belongs to **the first category**, as seen in Table 1 and Figure 1. In cubic structure, the main peak is d211. To the calculation of lattice parameter of cubic structure from known d211 diffraction, the next presented equation: a=sqrt(6*(d)^2)b was used.

In the case of X-ray diffraction patterns of samples with p6m hexagonal plane symmetry, **the second category of samples**, the 2Theta (2θ) values, and their derived "interlayer" distances (d spacing) and relative integral intensities of the peaks are written in the Table 1. A prominent d100 reflection around 2.2 Å, for 2θ angle value, which was assigned to p6m group of symmetry for hexagonal cell structure, is observed, in most of the samples. Lattice parameter (a_0) is depicted as the distance between 2 adjacent pore centres (and includes the pore wall as well) was calculated from d spacing of the most intense (100) peak in the XRD pattern, using formula: $a_0 = 2d_{100}/\sqrt{3}$.[12] Reduced a_0 is equivalent with a reduction in pore diameters. For more clarity, in Figure 2 it was represented the basic hexagon, where the main specific linear parameters were figured.

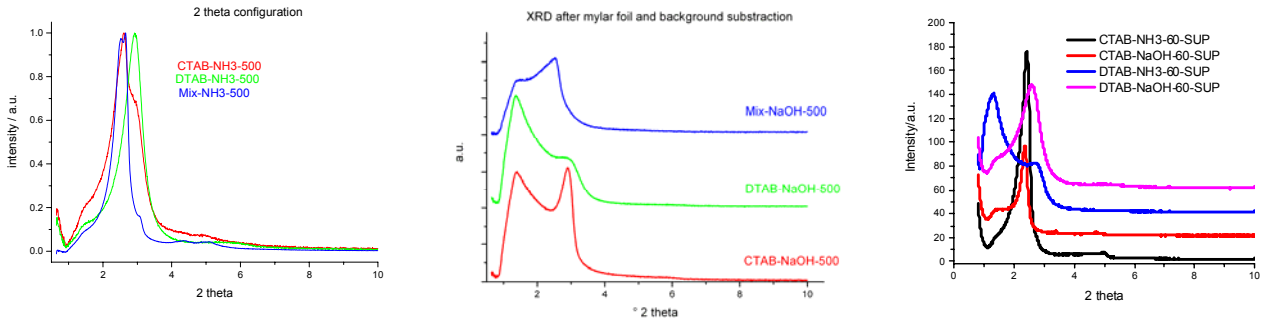

a) b) c)

Fig. 1 – Powder X-ray diffraction pattern of samples calcined at 500 °C (a and b) and of the xerogel ultra small particle fractions collected from supernatants (c).

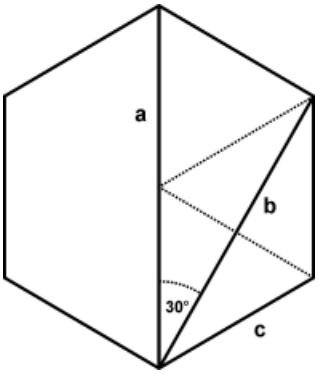

Fig. 2 – Hexagonal channel structure with distances **a**, **b**, and **c** between specific corners.

Table 1 shows the synthesized materials from DTAB series of samples as having shorter **a-**, **b-** and **c-** distances with respect to the analogous CTAB synthesised materials. This can be clearly explained by lower micelles size as a result of shorter carbon chain length of DTAB compared to CTAB. The MCM41 synthesized with CTAB showed (100), (110), and (200) reflections, whereas a less resolved pattern is obtained for sample, prepared from DTAB. The CTAB assisted samples presents XRD features, specifically the (100), (110), and (200) reflections, undoubtedly attributable to MCM41 type of hexagonal symmetry, whereas a less resolved pattern was obtained for DTAB series. The calculated values for the lattice spacing, d, in our present case, are comparative with the literature values.[5] For example, Vallet-Regi obtained the d(100) spacing of 39 Å and 36.5 Å for samples synthesized with C16TAB and the one with C12TAB, respectively.[5] For these samples's category, two main broad diffraction peaks are present. For example, at the sample DTAB-NH_3-60 is possible that the first broad peak fit (we used Pseudo-Voight function) with two overlapping components with 2θ maxima at 2.67° and 5.32°, corresponds to distances 33.1 Å and 16.6 Å. Direct distance of opposite corners is labelled as a-, and associates to first diffraction maximum. The second maximum, which was observable at the sample CTAB-NH_3-60 corresponds the b- distance. Relationships between a- and b- lengths could be written by equation: $b = \frac{\sqrt{3}}{2} * a$. The last diffraction peak with very weak intensity corresponds to the c – length of hexagon side of the structure. This parameter is one half of the a – parameter. At the majority of the samples are observable only diffraction peaks which can be attributed to a- and c- length. For the CTAB-NH_3-700 sample only the first broad peak was observed, as composed by two components – the peaks with 2θ maxima at 2.68° and 3.17°. These angles could be recalculated to 33Å and 27.8Å, respectively. Both values can be described with good precision by the above equation, too. We have calculated for this sample, the lattice parameter (a_0) as belonging to both hexagonal symmetry to and cubic as well, as based on the literature and to our peaks widths and positions, so we may assume there is a mixture of phases. At the diffractogram of the sample DTAB-NH_3-700 the peaks corresponding to a- and c- distances were observed.

The third category is the samples with **no calculated plan symmetry** or probably with a mixture between cubic and hexagonal phases. For example, for the NaOH-500ºC prepared samples, the XRD pattern (shown in Figure 1) the structure is partly degraded, yet not fully collapsed. Therefore, there is at least a local hexagonal ordering of the pores. **The last category** belong to the samples were no diffraction was observed. In the case of both samples (CTAB-NaOH -700 and DTAB-NaOH -700 (n.o.)) prepared in presence of sodium hydroxide and finally heated to 700°C no diffractions are visible in the studied area. This can be due to the presence of residual sodium ions in the silica structure. These ions act as modifier, which significantly reduces recrystallization temperature of the amorphous silica matrix.[14,15] This leads to collapse of the hexagonal structural motif of the MCM41 type samples.

DISCUSSION

In the previous reported studies,[7–11] in order to determine the structure of the mesoporous materials on a local scale (the short-range ordering), diffraction methods with electron microscopy methods were combined. Accordingly, a hexagonal closed pore packing can be considered on a local scale, around the centre of the spherical particle.[9] Pauwels et al also admitted a different XRD pattern for the spherical MCM-41 (the diffraction peaks of the XRD patterns are very broad) comparatively with the regular MCM-41 (which have sharp peaks).[8] They proposed 3 different theories[7]. One of the models is assuming saying that the pore channels, having the constant diameter, are radially propagating from the particle

center to the edge. Such as an extra pore is introduced when the distance between 2 neighboring pores become large enough. For the spherical particles, several Bragg peaks at low angles are observed (as it is typical for MCM-41) while the peaks are much broader. At the border of this spherical particle, distinct domains with ordered channels perpendicular to the surface could be differentiated. In this case, the first peak represents the nearest-neighbor distance. The ordering is quite good on a local scale (i.e. the short-range order). On the other side, the ordering on a larger scale (long range order), represented by the second and third neighbor peaks, is poor (as the results are in a broad, overlapping lines, in the XRD pattern). At this point, they considering a spherically symmetric model of pores, as follow: based on their proposed model, this hexagonal symmetry can only be observed in the middle part of the particles. At the sides of the particles, the pores are aligned in a plane perpendicular to the electron beam, which reveals the local arrangement of the pores at the sides. [7] In Table 1, the diffraction pattern assignment for the xerogels and calcined samples are presented: "*n.c.*" a_0 was not calculated due to indexation uncertainty; *"m.",* the Mix-NH3-500 sample is "mixture" of cubic and hexagonal phases; "*i."* two-phase sample – diffraction intensities are calculated together, as they were measured; "*u."* probably hexagonal with some "*unidentified"* diffractions; the relative intensity was determined as peak integral intensity.

Table 1

The X ray diffraction features assignment and the calculated lattice parameters

Sample	**a_0 [Å]**	**2theta [°]; d [Å]; relative intensity**				
Ia3d cubic symmetry		**(211)**	**(220)**	**(332)**		
CTAB-NH_3-60	91.37	2.37; 37.3; 100	2.63; 33.5; 30	4.67; 18.9; 0.5		
CTAB-NH3-500	82.86	2.61; 33.83; 100	2.96; 29.82; 18	4.93; 17.91; 1		
CTAB-NH_3-700 *(m.)*	80.83	2.68; 33.0; 100	3.17; 27.8; 7			
Mix-NH3-500 (*m., i.)*	81.27	2.66; 33.18; 41	3.08; 28.64; 6	4.92; 17.94; 5		
P6m hexagonal plane symmetry		**(100)**		**(110)**	**(200)**	**(210)**
CTAB-NH_3-700 *(m.)*	38.1	2.68; 33.0;100			3.17; 27.8; 7	
CTAB-NaOH-60	41.68	2.44; 36.1; 100			5.13; 17.2; 4	
CTAB-NaOH-60-sup (*u.)*	43.09	2.37; 37.32; 100	3.39; 26.08; 3		4.7; 18.77; 3	6.81; 2.98; 1
CTAB-NaOH-500	35.56	2.86; 30.8; 100			5,7; 15,3; 1	
DTAB-NH_3 -60	38.22	2.67; 33.1; 100			5.32; 16.6; 3	
DTAB-NH3-500	34.79	2,88; 30.63;100			5.7;15.53;3	
DTAB-NH_3 -700	32.79	3.11; 28.4; 100			6.07; 14.5; 4	
DTAB-NaOH -60	39.14	2.60; 33.9; 100			5.48; 16.1; 4	
DTAB-NaOH -60-sup	39.10	2.61; 33.86; 100			5.2; 17.06; 2	
Mix-NH3-500 (*m.)*	40.40	2.52; 34.98; 100		4.37; 20.20; 3	5.11; 17.27;1	
CTAB-NH_3-60-sup *(n.c.)*		2.44; 36.12; 100	3.9; 22.66; 1	4.49; 19.65; 4	4.97; 17.78; 3	
DTAB-NH_3-60-sup *(n.c.)*		2.77; 31.83; 100				
DTAB-NaOH -500 *(n.c.)*			2.81; 31.4; 100			
Mix-NaOH -500 *(n.c.)*		2.43; 36.2; 100				

In another study, Lebedev and his co-workers admits that the XRD interpretation is not easy as the large unit cells lead to diffraction peaks in the small-angle region. They are concluding that even if, in general, a broad peak is associated with a less ordered material, in the present case (of MCM type materials where the molar ratio TEOS: alcohol = 1:58) the broadening is created by a second diffraction signal. [10] In another work they have also concluded that, the spherical MCM-41 particles consist of a mixture of cubic and hexagonally arranged pores. The cubic structure and radial pores grown on the surfaces of a truncated octahedron. [8] In a newer study, they are explaining it like bundles of MCM-41 growing on the surface of a truncated MCM-48 nucleus, acting as the core of the spherical particles. [11]

In this context, we have observed that our synthesized samples as well contain a mixture of phases; variation was achieved by using different directing agents and different catalysts. Comparing the two catalysed groups of samples, for the ammonia catalysed samples, numerous diffractions peaks were observed which were attributed to hexagonal and cubic plane symmetry. In the meantime, within the sodium hydroxide catalysed group of samples, the majority of them presented either not indexed or not at all diffraction lines. By comparing the two templating agents, a less resolved pattern is obtained for the sample prepared with DTAB, compared those with CTAB. The calculated lattice parameter for the hexagonal cell structure was comparable with the literature values for MCM-41 type of materials[5] and it is decreasing with the increase of calcination temperature. The calculated lattice parameter for the hexagonal cell structure is decreasing with the decrease of the alkyl chain length.

EXPERIMENTAL

1. Sample synthesis

Chemicals: tetraethyl orthosilicate (TEOS), (99%, for analysis, Fluka); 2-methoxyethanol (Sigma-Aldrich, 99.8%); NH_4OHaq (25%, SC Silal Trading SRL); NaOH (Chemopal); hexadecyl-trimethylammonium bromide (cetyl-trimethylammonium bromide) (Sigma-Aldrich); n-dodecyl-trimethyl-ammonium bromide (Merck). In the present work, we have used 2-methoxyethanol as co-solvent. The molar ratios of the reactants were TEOS / 2-methoxyethanol / H_2O / catalyst (NH_3 or NaOH) / directing agent = 1:58:144:11(0.31):0.3 respectively. Six xerogel samples were prepared in sol-gel synthesis by using CTAB, DTAB or their equimolecular mixture, either in presence of ammonia or NaOH, by using a previous reported procedure.[15] The directing agent (CTAB or DTAB, or their mixture, CTAB+DTAB) was dissolved in a mixture of distilled water and 2-methoxyethanol. Subsequently the catalyst (ammonia or NaOH) was added. The mixtures were vigorously stirred in a closed vessel at room temperature for 30 min. Then, 10 mL of TEOS sol–gel precursor was slowly dripped in, and vigorous stirring was continued for 24 h. The resulted suspension was washed several times with distilled water in ultrasonic bath (and then centrifuged at 3500 rpm, after each washing step) until the pH of the supernatant was close to neutral. The first supernatant was kept and treat in the same manner as the precipitate material; the samples resulted from the first supernatant were labelled with "SUP". Ethanol was added to the resulted and subsequently separated precipitate and left for 24 h. After that, the material was dried at 60 °C and the samples were labelled as "60". A part of each dried sample has been further heated up to 500 °C, another part to 700 °C for 6 h, and the corresponding samples were labelled as "500" and "700" respectively (see all the samples listed in Table 1).

2. Sample characterization method

X-ray powder diffraction (XRD) measurements were performed on Panalytical X'Pert Pro MPD diffractometer equipped with Cu-anode (Cu Kα; λ=0.15418 nm) and X'Celerator detector. Measurements were done at room temperature in transmission mode using Mylar foil over an angular range from 0.65 to 10° in 2θ.

CONCLUSIONS

The XRD measurements revealed that our synthesised materials have ordered mesoporous structure, mainly attributable to hexagonally pore symmetry. Based on the reported, dedicated studies of electron diffractions [8-13] regarding this complex type of materials and based on our X-ray diffraction studies, presented here, we assume that, either a cubic and hexagonal short-range order or a mixture of hexagonal and cubic phases can be found in the final obtained materials. We did not found any unequivocal relation between composition of reaction mixture and the structure. The CTAB synthetized samples preferably create cubic structure whereas the DTAB synthetized samples create preferably hexagonal structure. Mixtures samples create probably non homogeneous mixture of both structures. It can be observed the shrinkage of the mesostructured unit cells, as these are decreasing from xerogels to the calcined samples, and also are decreasing with the increase of the calcination temperature.

Acknowledgement. Authors thank the Roumanian Academy and the Inter-Academic Exchange Program between Czech Academy of Sciences and Roumanian Academy.

REFERENCES

1. H. Xu, Y. Li, Z. Yang, Y. Ding, C. Lu, D., Li and Z. Xu, *Int. J. Appl. Ceram. Tec*., **2012,** *9*, 1112-1123.
2. H. Zhang, J. Wu, L. Zhou, D. Zhang and L. Qi, *Langmuir,* **2007**, *23*, 1107-1113.
3. K. Yano, Toyota CRDL, *Tech. J. R&D*, **2004**, *40*, 28-35.
4. J. Goworek, A. Kierys, M. Iwan and W. Stefaniak, *J. Therm. Anal. Calorim.*, **2007**, *87,* 165–169.
5. M. Vallet-Regi, A. Ramila, R. P. del Real, and J. Perez-Pariente, Chem. Mater., **2001**, *13*, 308-311.
6. Y. Yu-Xiang, Y. Hai-Ping, S. Jian-Guo, H. Zheng, L. Xiang-Nong and C. Ya-Ru, *J. Am. Ceram. Soc*., **2007**, *90*, 3460-3467.
7. B. Pauwels, G. Van Tendeloo, C. Thoelen, W. Van Rhijn and P. A. Jacobs, *Adv. Mater.*, **2001**, *13*, 1317-1320.
8. G. Van Tendeloo, O. I. Lebedev, O. Collart, P. Cool and E. F. Vansant, *J. Phys. Condens. Matter*., **2003**, *15*, S3037.
9. S. Liu, P. Cool, O. Collart, P. Van Der Voort, E. F. Vansant, O. I. Lebedev, G. Van Tendeloo and M. Jiang, *J. Phys. Chem. B*, **2003**, *107*, 10405-10411.
10. O. I. Lebedev, G. Van Tendeloo, O. Collart, P. Cool and E. F. Vansant, *Solid State Sci.*, **2004**, *6*, 489–498.
11. O. I. Lebedev, S. Turner, S. Liu, P. Cool and G. Van Tendeloo, *Nanoscale*, **2012**, *4*, 1722-1727.
12. S. Hudson, D. A. Tanner, W. Redington, E. Magner, K. Hodnett and S. Nakahara, *Phys. Chem. Chem. Phys.*, **2006**, *8*, 3467–3474.
13. NIIR Board of Consultants and Engineers, "The Complete Book on Glass and Ceramics Technology", Asia Pacific Business Press Inc., India, 2005.
14. S. A. M. Abdel-Hameed and A. M. El Kady, *J.A.R.*, **2012**, *3*, 167–175.
15. A. M. Putz, C. Savii, C. Ianăşi, D. Dudás, K. N. Székely, J. Plocek, P. Sfârloagă, L. Săcărescu and L. Almásy, *J. Porous Mater*., **2015**, *22*, 321-331.